ЖЭТФ, 2005, том 127, вып. 1, стр. 18–26

ELECTRON-FORBIDDEN ENERGY GAP OF HYDROGEN IN A WIDE PRESSURE INTERVAL

A. G. Khrapak *

Institute for High Energy Density, Russian Academy of Sciences
125412, Moscow, Russia

K. Yoshino

Department of Electronic Engineering, Graduate School of Engineering, Osaka University
565-0871, Osaka, Japan

Submitted 24 June 2004

A simple model is used for estimation of the bottom energy of the electron conduction band and the electron-forbidden gap energy. It is shown that electrons in liquid hydrogen are localized not in the electron bubbles as was considered previously but in molecular negative ions surrounded by voids of radius about 0.5 nm. The conductivity of fluid hydrogen at not very high pressures is connected to transfer of positively charged clusters and negatively charged bubbles. As the pressure and density increase, molecular dissociation occurs and electron localization on atoms becomes more favorable, also with creation of void around atomic negative ions. At a sufficiently high concentration of atoms, the probability of the tunnel transition of an electron from one atom to another becomes close to unity, the energy level of the negative ion degenerates in the band, and the conductivity is caused by the transfer of these quasifree electrons. It is supposed that this charge transfer mechanism may play important role in the region of the fluid hydrogen metallization.

PACS: 72.20.-i, 52.27.Gr

1. INTRODUCTION

Investigations of hydrogen behavior in the solid, liquid, and plasma state are of significant importance from both scientific and technological standpoint. They are important in astrophysics because hydrogen is the most abundant chemical element, which constitutes about 3/4 of the Universe matter. Jupiter and Saturn together contain over 400 Earth masses, most of which is hydrogen, heated and compressed to high temperatures and pressures. Hydrogen is fluid at these conditions. The convective motion of electrically conducting hydrogen produces the magnetic field of giant planets by the dynamo action (see [1] and references therein). The knowledge of the equation of state and physical properties of hydrogen and its isotopes is very important for successful solution of the problem of the inertial nuclear fusion. An intriguing possibility of metastable metallic and even superconducting phases of solid hydrogen at ambient pressure has been predicted [2].

In 1935, Wigner and Huntington predicted that molecular diatomic hydrogen would undergo a transition to a metallic state at an imposed pressure of about 25 GPa [3]. Current predictions are in a range close to 300 GPa [4]. But despite unrelenting experimental assault, dense solid hydrogen shows no evidence of metallic behavior [5]. In the fluid, electric conductivity measurements under multiple-shock compression indicate that hydrogen becomes metallic at pressures about 140 GPa, ninefold the initial fluid density, and temperature about 3000 K [6–10]. Electric conductivity has also been measured under single-shock compression up to 20 GPa and 4600 K [11]. Those experiments show that conductivity is thermally activated similarly to the semiconducting fluid and becomes greater than 1 $(\Omega \cdot \mathrm{cm})^{-1}$ at 200 GPa and 400 K. The pressure dependence of the conductivity measured in [9] is shown in Fig. 1. The change in slope at 140 GPa is indicative of the transition to the metallic state. An analysis of the measurements in the range 93–120 GPa (semiconducting regime) resulted in the equation typical of

*E-mail: khrapak@mail.ru

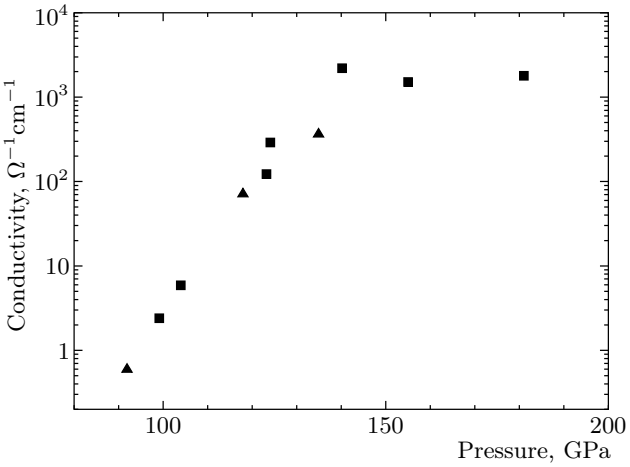

Fig. 1. Electric conductivity of H_2 and D_2 as a function of pressure [8]. The slope change at 140 GPa is the transition from semiconducting to metallic fluid. Experimental points: triangles [14], squares [11]

liquid semiconductors,

$$\sigma = \sigma_0 \exp\left[-E_g(\rho)/2k_BT\right], \tag{1}$$

where σ is the electric conductivity, σ_0 weakly depends on the density ρ, $E_g(\rho)$ is the density-dependent electron band gap of the fluid, k_B is the Boltzmann constant, and T is the temperature. If the temperature dependence of conductivity is related to transition of electrons from the ground state to the continuous spectrum, then E_g coincides with the ionization potential of the hydrogen molecule in matter. The results of the least-square fit of the experimental data to Eq. (1) are

$$\begin{aligned} &E_g(\rho) = 1.22 - 62.6(\rho - 0.300), \\ &\sigma_0 = 90, \quad 0.290 \le \rho \le 0.319, \end{aligned} \tag{2}$$

where $E_g(\rho)$ is in eV, ρ is in mol/cm^3, and σ_0 is in $(\Omega \cdot \mathrm{cm})^{-1}$. We note that a value 200–300 $(\Omega \cdot \mathrm{cm})^{-1}$ is typical of liquid semiconductors [12]. The band gap was also estimated as $E_g = 11.7 \pm 1.7$ eV at the point $\rho = 0.13 \pm 0.005$ mol/cm^3 in the single-shock experiments [11]. The metallization density is defined to be the density at which the mobility band gap E_g is reduced by pressure to $E_g \sim k_BT$, at which point E_g is filled in by fluid disorder and thermal smearing. We have $E_g(\rho) \approx k_BT$ at the density about 0.316 mol/cm^3 and the temperature about 2600 K (0.22 eV). Thus, fluid hydrogen becomes metallic at about 140 GPa and 2600 K via continuous transition from a semiconducting to metallic fluid.

The band gap E_g has been measured only for solid H_2 and D_2 at low temperatures (about 5 K) and low (saturation) pressures [13, 14]. The vacuum ultraviolet absorption spectra of these two hydrogen isotopes are practically identical. The low-energy component of the spectra below 15 eV was assigned to the Wannier exciton transitions. The analysis of the higher members of the Wannier series in [14] implies that $E_g \approx 14.7$ eV in hydrogen and $E_g \approx 14.9$ eV in deuterium. These values are close to the gas phase ionization potentials of the hydrogen molecules: $I_g = 15.43$ eV for H_2 and $I_g = 15.47$ for D_2. The knowledge of E_g allows estimating the energy of the bottom of the electron conduction band V_0. In fact, the molecular ionization potential in a dielectric matter, as it follows from the close-coupling approximation, is related to the gas phase ionization potential by

$$E_g = I_g + P_+ + V_0, \tag{3}$$

where P_+ is the polarization energy of the medium by a positive ion. For estimation of the value of P_+, the Born formula can be used

$$P_+ = -\frac{e^2}{2R_i}\left(1 - \frac{1}{\varepsilon}\right), \tag{4}$$

where R_i is the radius of the cavity where a point charge resides surrounded by a homogeneous liquid or solid with the dielectric constant ε. Usually, R_i is chosen equal to the crystallographic ionic radius or to the hard core radius of the neutral parent molecule. Good agreement with the results of the theoretical estimates of P_+ for solid rare gases [15, 16] may be achieved for

$$R_i = R_s, \quad R_s = \left(\frac{3}{4\pi N}\right)^{1/3}, \tag{5}$$

where R_s is the radius of the cell occupied by a molecule in the medium with the concentration of molecules N. Substitution of Eq. (5) in Eq. (4) gives $P_+ = 0.7$ eV for H_2 and $P_+ = 0.8$ eV for D_2. Thus, according to this estimation, the energy of the bottom of the electron conduction band V_0 is approximately equal to -0.05 eV in solid H_2 and $+0.20$ eV in solid D_2.

The sign and value of V_0 are determined by competition between the polarization and exchange interactions of an electron with molecules of the medium,

$$V_0 = T_e + P_e, \tag{6}$$

where $P_e < 0$ is the energy of the medium polarization by an electron and $T_e > 0$ is the minimum kinetic energy that a free electron can have in a system of short-range repulsive scatterers. With decreasing N, the relative contribution of the polarization interaction

increases, and V_0 must therefore also be negative in liquid and gas phases of hydrogen. In the ideal gas, the optical model [17] may be used for estimation of V_0,

$$V_0 = \frac{2\pi\hbar^2}{m} LN, \qquad (7)$$

where m is the electron mass and L is the electron–molecule scattering length. This implies that L must be negative and demonstrate a Ramsauer–Tawnsend minimum. The scattering length was obtained in spectroscopic investigation of the properties of electrons localized above the surface of solid hydrogen [18, 19]. The resonant energy of the electron transition between ground and excited surface states was found in this experiment to depend on the density N of H_2 molecules in the vapor phase. The linear density shift of the transition energy was interpreted in terms of the optical model (in full analogy with the Fermi shift of energy of high excited Rydberg atoms in a gas atmosphere) by means of Eq. (7). This gave the value $L = -0.14 \pm 0.04$ nm and negative V_0, which is in qualitative agreement with the previously discussed results of spectroscopic investigations of solid hydrogen. We note that the currently accepted value is $L = +0.067$ nm. Discussion of possible reasons of this discrepancy can be found in [19]. Most probably, discrepancy occurs because practically all measurements of the electron scattering length were performed at temperatures high enough for the rotational degrees of freedom to be excited. Only Zavyalov and Smolyaninov [18, 19] did their experiments at cryogen temperatures.

A negative value of V_0 indicates the absence of a potential barrier for penetration of an electron from the gas phase to bulk liquid or solid hydrogen. At first sight, this contradicts a number of well-known experimental facts. First, the possibility of the electron localization above the surface of condensed He, Ne, and H_2 is usually connected with the existence of a potential barrier for electrons at the surface of these three matters having small polarizability of atoms or molecules [20, 21]. Second, in the experiments on mobility of charge carriers in liquid [22–24] and solid [25–27] hydrogen, a very low mobility of negative charges (of the same order as or in some cases even less than the mobility of positive charges) was observed. The current interpretation of this effect supposes that just as in liquid and solid helium, the positive charges represent clusters (Atkins' snowballs [28]) consisting of a positively charged molecular ion surrounded by a layer of neutral molecules, and the negative charges in condensed hydrogen are electrons localized in bubbles or voids of several atomic sizes [21]. This interpretation also implies the existence of a sizable potential barrier of about 1–2 eV at the surface of the electron bubble. Third, irradiated solid hydrogen displays a number of interesting spectral features. Hydrogen mixtures containing tritium, when cooled below the temperature about 10 K, show additional lines in the fundamental absorption spectrum [29]. The new lines were interpreted as Stark-shifted molecular transitions whose appearance was caused by the presence of trapped charges of both signs in the lattice as a result of the ionizing tritium radioactivity. Proton- and γ-irradiated samples show the same features. The analysis of Stark shifts resulted in the conclusion that two species of each charge exist, one mobile and one less mobile. Each of the less mobile charge species is responsible for the induced absorption features. The mobile negative charge is thought to be a small polaron and its immobile counterpart is then an electron trapped in the form of a bubble [30]. In addition to the Stark-shifted features, a number of spectral features also attributed to trapped electrons have been observed in irradiated solid hydrogen (see, e.g., [31] and references therein). A simple square-well model for the electron bubble gives a good fit to the observed spectra only for an unreasonably large well depth $V_0 = 3.8$ eV [32].

One of the aims of the present work is to eliminate the aforementioned contradictions between different experiments. With the help of a simple model, we show that even in the case of a negative V_0 (but not very large in the absolute value), two-dimensional electron surface states may exist owing to the additional potential barrier at the surface, whose appearance is related to the different ranges of polarization and exchange forces. An important role of the polarization energy at the surface and interface was also reported for other dielectric and semiconducting systems [33]. Using the fact of the recently observed formation of the H_2^- ion in solid hydrogen [34–36], we conjecture that the low mobility of negative charges in condensed hydrogen is a result of the electron capture by a hydrogen molecule and bubble creation around it but not the result of the electron bubble creation. We assume that in the case of irradiated liquid and solid hydrogen, the availability of the admixture of hydrogen (deuterium) atoms is decisive and electrons are localized in H^- (D^-) surrounded by voids of a smaller size than in the case of H_2^- (D_2^-). Near the metallization pressure of hydrogen, considerable dissociation of molecules (about 10 %) occurs [8]. Electrons are localized in atomic negative ions. With increasing the pressure, overlapping of the neighboring atomic negative ion states should result in formation of

the extended electron band and lead to the insulator–metal transition. In this paper, results of our determination of the density dependence of V_0 and E_g are presented and compared with the results of the single-shock experiments.

2. ENERGY OF THE BOTTOM OF THE ELECTRON CONDUCTION BAND

In dense fluids and solids, the interaction between atoms and molecules plays an important role, optical model (7) is inapplicable for estimation of V_0, and more detailed consideration of Eq. (6) is necessary. The energy P_e of the polarization interaction of electrons with matter differs from the ion polarization energy P_+. Calculation performed for solid rare gases [16] are well fitted by

$$P_+ = -\frac{1}{a}\varphi_+\left(\frac{\alpha}{a^3}\right), \qquad \varphi_+(t) = \frac{3.154t - 3.860t^2}{1 + 2.55t - 4.750t^2}, \tag{8}$$

$$P_e = -\frac{1}{a}\varphi_e\left(\frac{\alpha}{a^3}\right), \qquad \varphi_e(t) = \frac{4.966t + 0.924t^2}{1 + 3.244t + 0.957t^2}, \tag{9}$$

where $a \approx 1.2R_s$, α is the atomic or molecular polarizability, and t satisfies the conditions $0 < t < 0.2$. Approximation (8) coincides numerically with the calculation data in [15] and Born formula (4). It is well known that for helium isotopes and other rare gases, the value of V_0 depends essentially on the atomic density and is practically independent of the isotope composition, aggregative state, and the type of the crystal structure [37]. Therefore, there is good reason to believe that Eqs. (8) and (9) can be used for solid and fluid hydrogen and deuterium. The results of estimation of the polarization energy of positive ions and electrons near the triple point of H_2 and D_2 are listed in the Table.

For estimation of the minimum electron kinetic energy T_e, it is necessary to specify the short-range part of the interaction potential. The interaction of an electron with an atom or molecule in the vacuum can be qualitatively described by a simple model potential shown in Fig. 2 [38, 39],

$$V(r) = \begin{cases} \infty, & r \le R_c, \\ -\dfrac{\alpha e^2}{2mr^4}, & r > R_c. \end{cases} \tag{10}$$

Results of estimation of the characteristic energies of H_2 and D_2 near their triple points: the positive ion P_+ and the electron P_e polarization energy, the minimum electron kinetic energy T_e, the energy of the bottom of the electron conduction band V_0, and the electron mobility gap or ionization potential E_g. All values are in eV

	Hydrogen		Deuterium	
	Liquid	Solid	Liquid	Solid
P_+	−0.67	−0.78	−0.78	−0.91
P_e	−1.08	−1.26	−1.26	−1.48
T_e	0.95	1.09	1.09	1.27
V_0	−0.08	−0.16	−0.16	−0.18
E_g	14.68	14.49	14.53	14.38

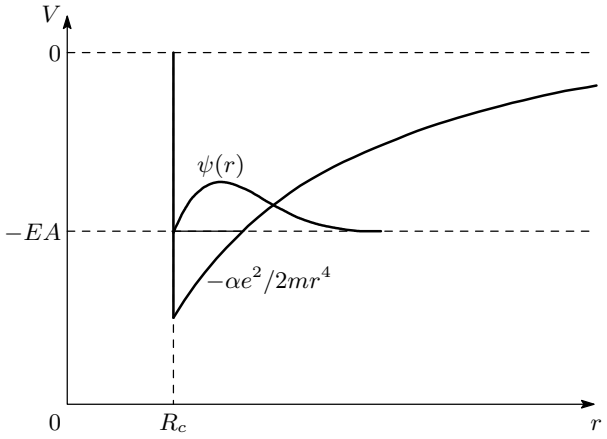

Fig. 2. A model potential for the electron–atom or electron–molecule interaction $V(r)$ and the electron wave function $\psi(r)$ in the negative ion

The only unknown parameter of the potential, the solid core radius R_c, is fitted as follows. In the case where a stable negative ion of the corresponding species exists (as is the case with H^-), the value of R_c is sought with which the solution of the Schrödinger equation with potential (10) gives the correct value of the electron affinity EA. The atomic hydrogen has EA = 0.754 eV [40], which results in $R_c = 0.032$ nm. A negative ion of molecular hydrogen does not exist in the vacuum. In this case, it is possible to use the known relation between R_c, α, and the electron scattering length L [41],

$$L = \sqrt{\frac{\alpha}{a_0}}\ \operatorname{ctg}\sqrt{\frac{\alpha}{a_0 R_c^2}}\,, \tag{11}$$

where a_0 is the Bohr radius. Substitution of the value

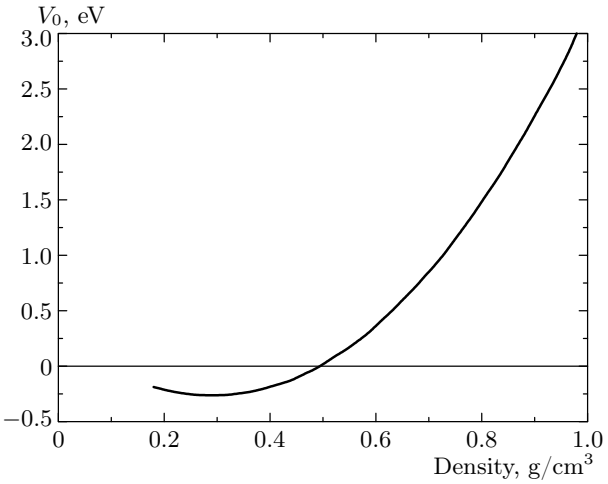

Fig. 3. The energy of the bottom of the electron conduction band V_0 in fluid D_2 as a function of the density ρ

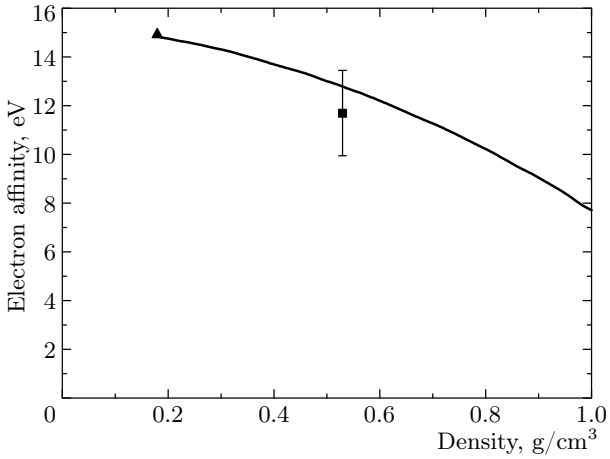

Fig. 4. The electron-forbidden energy gap in fluid D_2 as a function of the density ρ

$L = -0.14$ nm in Eq. (11) results in $R_c = 0.052$ nm. This value of R_c seems quite reasonable because in the scattering of two closed atoms, it has to be twice the atomic R_c, but correlation in positions of the atoms in the molecule slightly reduces the value of R_c.

Knowing the radius of the molecular hard core, it is possible to calculate the value of zero-point electron energy T_e. An approach commonly used for this is based on the Wigner–Seitz model [15, 37, 42]. In this model, the medium is divided into equivalent spheres of radius R_s. Each sphere contains a hard core of radius R_c in its center. A free electron may be in any cell with equal probabilities. Therefore, the electron wave function $\psi(r) \sim r^{-1}\sin[k(r - R_c)]$ and $\psi'(r)$ must be continuous at the cell boundaries, which is possible only if $\psi'(R_s) = 0$. This gives

$$T_e = \frac{\hbar^2 k^2}{2m}, \quad kR_s = \operatorname{tg}\left[k(R_s - R_c)\right]. \qquad (12)$$

The results of estimations of T_e and the values of V_0 and E_g following from Eqs. (6) and (3) are also listed in the Table. It follows that our estimation of the ionization potential E_g in solid hydrogen is in a good agreement with spectroscopic measurements [14] and the bottom of the electron conduction band V_0 is negative in all the cases considered.

This model allows determining the dependence of V_0 and E_g on the fluid density ρ. The results of our calculations are shown in Figs. 3 and 4. V_0 has a minimum at the density about 0.3 g/cm^3 and becomes positive at about 0.5 g/cm^3. Such behavior is typical of all fluid rare gases having negative V_0 under ambient conditions. The forbidden energy gap decreases with density and within the experimental errors coincides with E_g produced by single-shock compression at the point 0.53 g/cm^3.

3. SURFACE POTENTIAL BARRIER AND LOCALIZATION OF ELECTRONS ON THE HYDROGEN SURFACE

For liquids with a positive value of V_0 (for example, helium and neon), the electron transfer from the vacuum into the liquid is hampered by this barrier. An electron approaching the surface from the vacuum nevertheless feels the influence of its positive image charge inside the liquid. The potential of this attractive image force above the surface is given by

$$V(z) = -\frac{Qe^2}{z}, \quad Q = \frac{\varepsilon - 1}{4(\varepsilon + 1)}, \qquad (13)$$

where z denotes the coordinate perpendicular to the surface and ε is the dielectric constant of matter. The attraction by the image force and the barrier given by V_0 lead to a bound surface state [20, 21]. The electron is, however, still partially free to move along the surface and has high mobility in these directions. For liquid helium, the potential barrier $V_0 \sim 1$ eV is high in comparison with the binding energy of the localized electron. Therefore, it is possible to put $V_0 = \infty$ with a good accuracy and to take the presence of the interface into account by the boundary condition of the wave function $\Psi|_{z=0} = 0$. The attractive potential then gives rise to a hydrogen-like wave function with the Bohr radius becoming a_0/Q. The energy levels correspond to

the Rydberg series and the electron energy spectrum is given by

$$E_n(\mathbf{k}) = \frac{\hbar^2 \mathbf{k}^2}{2m} - \frac{mQ^2e^4}{2\hbar^2 n^2}, \quad n = 1, 2, \ldots, \qquad (14)$$

where $\mathbf{k}$ is a two-dimensional wave vector of the electron parallel to the helium surface. Owing to small polarizability of helium ($Q \approx 1/144$), the ground state binding energy is also small ($E_1(0) \approx 7.5$ K $\ll V_0$) and the assumption $V_0 = \infty$ is quite reasonable in this particular case. The electron is localized at the distance of the order of 100 nm from the surface and therefore the true behavior of the interaction potential at the distance of the interatomic order from the surface is not very important. The frequencies of the 1–2 and 1–3 transitions correspond to 125.9 and 148.6 GHz, respectively.

In the case of condensed hydrogen, the situation is different. As we showed above, V_0 is negative in both liquid and solid hydrogen, and at first sight, the surface electron localization is impossible. Such states were nevertheless observed [18, 19, 43, 44]. We now consider the spectroscopic measurements with surface electrons on solid hydrogen surfaces in more detail [19]. A tunable laser source enabled observing the photoresonance of the surface electrons when changing the potential of the lower electrode U (and, consequently, the confining electric field E) altered the electron spectrum. The photoresonance signal amplitude depended linearly on the laser intensity and on the surface charge density. The transition frequency in the limit of zero electric field E and hydrogen gas pressure P was equal to 3.15 ± 0.05 THz. As in the case of similar experiments for electrons over ^{3}He and ^{4}He [45, 46], the energy spectrum can be approximated by introducing the Rydberg correction δ into Eq. (14),

$$E_n(0) = -\frac{mQ^2e^4}{2\hbar^2(n+\delta)^2}, \qquad (15)$$

where δ is independent of n. Measurements of δ for ^{3}He and ^{4}He gave -0.014 and -0.022, respectively, while $\delta = -0.11$ was obtained for solid hydrogen [18, 19]. As we already mentioned, Zavyalov and Smolyaninov found that for electrons over solid hydrogen and deuterium, the transition frequencies depend strongly on the vapor density. Analysis of this dependence allowed determining the scattering length L that we use in our estimations. That the scattering length is negative is important evidence that V_0 is negative.

To understand why creation of the localized surface states is possible in the case of negative V_0, we consider the interaction of an electron with the hydrogen surface in more detail. The interaction potential $V(z)$ is shown schematically in Fig. 5. Inside condensed hydrogen, the potential energy of the long-range polarization interaction P_e is determined, for example, by Eq. (9). Approaching the surface, P_e increases. At the surface, it is tied continuously to the image force potential, which is determined by Eq. (13) far from the surface. An electron located just at the surface interacts with a half of the molecules with which it interacts in the bulk matter. It is therefore reasonable to assume that at the surface, the polarization energy is approximately equal to $P_e/2$. In addition to the polarization interaction, there is a short-range exchange interaction of the electron with electrons of hydrogen molecules, which results in the shift of the free electron energy V_0 by a positive value T_e. The dependence of $T_e(z)$ is significantly more abrupt than of $P_e(z)$. We approximate it by the step function. The resulting surface potential depicted in Fig. 5 by solid line represents the potential barrier for electrons penetrating from the vacuum side. It is obvious that if V_0 is not too small, the surface electron localized states may exist.

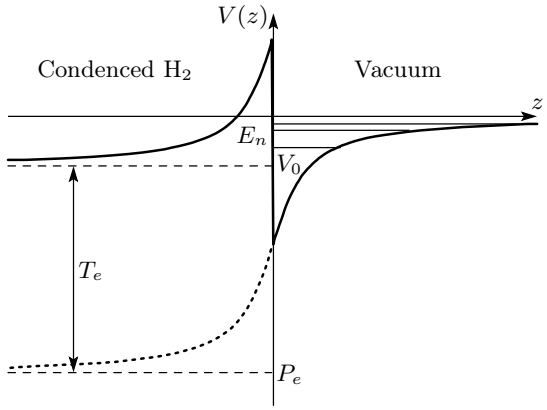

Fig. 5. Schematic arrangement of the electron interaction potential at the surface of condensed hydrogen

For determination of the surface electron energy spectrum, we use an even simpler potential. Outside hydrogen, it coincides with the image force potential (13) down to $z = R_c = 0.052$ nm. At shorter distances, the potential is considered to be constant, $V(z) = V(R_c)$. Inside hydrogen, the potential is also considered to be constant, $V(z) = V_0 - P_e/2$. Solution of the Schrödinger equation gives the spectrum in Eq. (15) with $\delta \approx -0.2$ that is practically independent of n. For the model thus simplified, the agreement with the experimental value $\delta = -0.11$ is quite satisfactory. It is worthwhile to note that we used the continuity conditions

$$\psi(-0) = \psi(+0), \quad m_{eff}^{-1}\psi'(-0) = m^{-1}\psi'(+0) \qquad (16)$$

for the electron wave function $\psi(z)$ [47], where m_{eff} is the electron effective mass. In liquid helium, $m_{eff} \approx m$ and both masses are cancelled in Eq. (16). In solid hydrogen, $m_{eff} \approx 0.2m$ [48]. The sudden change of the electron effective mass at the hydrogen surface results in a significant increase of the surface electron binding energy.

4. THE STRUCTURE AND ENERGY SPECTRUM OF ATOMIC AND MOLECULAR NEGATIVE IONS IN CONDENSED HYDROGEN

The electron affinity to atoms and molecules increases in condensed dielectrics in comparison with its value in the vacuum [49–53]. This effect was observed by Lukin and Yakovlev [49] and Sowada and Holroyd [50] in experiments on conductivity of solutions of molecular oxygen in different dielectric liquids. Such solutions were exposed to short X-ray radiation pulses. This resulted in ionization of the solvent and a sharp growth of the conductivity. Then the electrons were localized at the neutral oxygen molecules with creation of the negative ions O_2^-. After that, the conductivity dropped down abruptly because the mobility of heavy O_2^- ions is several orders less than the mobility of free electrons. Then the laser pulse in the visible spectrum was produced. If the laser frequency exceeded some threshold value, then the photodetachment occurred, accompanied by new growth of the conductivity. The photodetachment energy was found to be significantly higher than the electron photodetachment energy from the oxygen molecule in the vacuum (the difference was more than 1 eV). This effect is the result of a strong polarization interaction of the bound electron with atoms or molecules of the solvent. A more detailed discussion of this effect can be found in [51–53].

As a result of the irradiation or thermal dissociation, some amount of atomic hydrogen may be present in condensed molecular hydrogen. We therefore perform our estimations for both atomic and molecular negative ions. At the moment of the electron transition to the level of a negative ion, surrounding matter can be considered undisturbed. The electron binding energy in the negative ion can then be estimated from the solution of the Schrödinger equation with a potential slightly different from that in Eq. (10) and Fig. 2. It is represented in Fig. 6. At the surface of the void surrounding the negative ion with $R = R_s$, the interaction potential varies stepwise by the value T_e. The

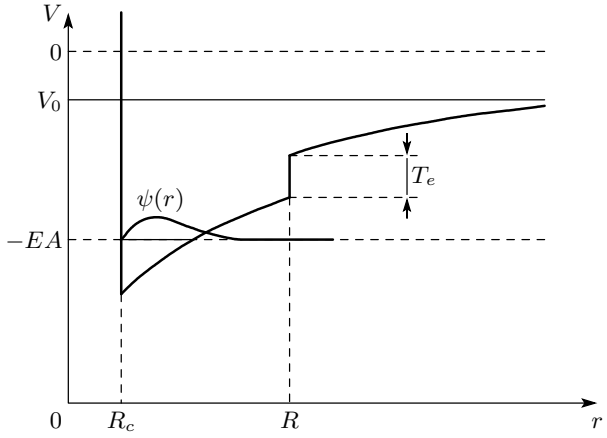

Fig. 6. A model potential for the electron–atom or electron–molecule interaction $V(r)$ and the electron wave function $\psi(r)$ in the negative ion inside a bubble of radius R

estimation of the electron affinity gives, for example, EA $\approx$ 1.33 eV for H^- in liquid hydrogen at the triple point and EA $\approx$ 1.42 eV for D^- in solid deuterium also at the triple point. A continuous red emission spectrum was observed during proton-beam irradiation of solid D_2 and H_2, maximizing near 830 nm (1.49 eV) [31, 54]. We believe that the electron attachment to D and H is responsible for this emission. Similar estimation shows that the electron affinity to the hydrogen molecule in undisturbed hydrogen is negative. Hence, the radiative formation of the H_2^- and D_2^- ions is impossible. With increasing the fluid density, the electron affinity increases. The results of our calculation of the electron affinity to atomic deuterium in fluid molecular deuterium are shown in Fig. 7.

After the atomic negative ion formation, the interaction of its outer electron with surrounding matter results in the creation of a void around the ion, with the electron energy decreasing. At the bubble radius about 0.5 nm, the electron energy shift is about 0.15–0.20 eV. With the potential barrier at the surface of the void being of order of $P_e/2$, the electron detachment energy is approximately equal to 1.9 eV for H^- in liquid H_2 and 2.2 eV for D^- in solid D_2. The last value is somewhat different from the experimentally measured value about 3.1 eV of the electron bound-free transition energy in proton-irradiated solid deuterium [32]. Nevertheless, we believe that photodetachment of electrons from the D^- ions may be responsible for this ultraviolet absorption spectrum and suppose that a more refined calculation of the hydrogen negative ion spectrum is capable of improving the agreement with experiment. Creation

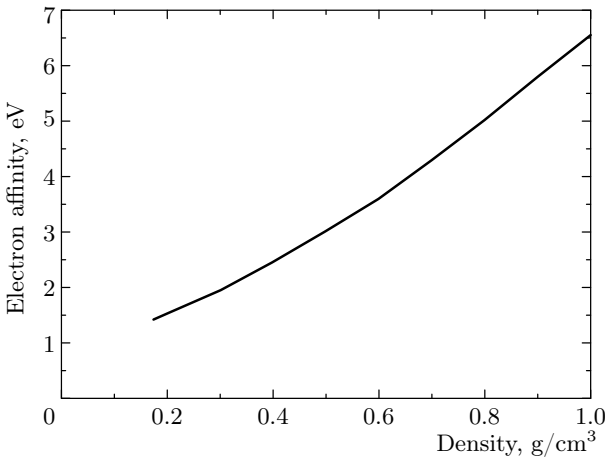

Fig. 7. Electron affinity to atomic deuterium in fluid deuterium as a function of density

of negative H_2^- and D_2^- ions also becomes possible inside voids of a sufficiently large radius. For example, the electron detachment energy for the D_2^- ion in the void of diameter 0.5 nm in solid D_2 is approximately equal to 1.3 eV. Close values are valid for H_2^- in liquid and solid H_2, and for D_2^- in liquid D_2. This allows us to suppose that low mobility of negative charges in liquid and solid hydrogen [22–27, 39] is related to the electron localization in molecular or atomic (when dissociation of molecules occurs) negative ions surrounded by bubbles or voids.

5. CONCLUSION

A simple model for estimation of the bottom energy of the electron conduction band V_0 and the forbidden energy gap E_g was proposed based on the experimental investigation of the exciton absorption spectrum in condensed hydrogen. Estimation of E_g is in a good agreement with the values obtained in the measurements of conductivity by single-shock wave experiments. It was shown that electrons in liquid hydrogen are localized not in the electron bubbles, as was considered previously, but in molecular negative ions surrounded by voids of radius about 0.5 nm. The conductivity of fluid hydrogen at not very high pressures is related to the transfer of heavy complexes — positively charged clusters and negatively charged bubbles. With increasing pressure and density, the molecular dissociation occurs and the electron localization on atoms becomes more favorable, also with the creation of void around atomic negative ions. At a sufficiently high concentration of atoms, the probability of a tunnel transition of an electron from one atom to another becomes close to unity, the energy level of the negative ion degenerates in the band, and the conductivity is caused by the transfer of these quasifree electrons. This mechanism of charge transfer may play an important role in the region of fluid hydrogen metallization.

A. G. K. gratefully acknowledges support from Osaka University, the Russian Foundation for Basic Research, and Deutsche Forschungsgemeinschaft. This study was supported by the Presidium of the Russian Academy of Sciences (Program on thermophysics and mechanics of extreme energy stimulation).

REFERENCES

1. W. J. Nellis, Planet. Space Sci. **48**, 671 (2000).
2. N. W. Ashkroft, Phys. Rev. Lett. **21**, 1748 (1968).
3. E. Wigner and H. B. Huntington, J. Chem. Phys. **3**, 764 (1935).
4. P. P. Edwards and F. Hensel, Nature **388**, 621 (1997).
5. R. J. Hemley and H. Mao, J. Low Temp. Phys. **122**, 331 (2001).
6. S. T. Weir, A. C. Mitchell, and W. J. Nellis, Phys. Rev. Lett. **76**, 1860 (1996).
7. V. Y. Ternovoi, A. S. Filimonov, V. E. Fortov et al., Physica B **265**, 6 (1999).
8. W. J. Nellis, S. T. Weir, and A. C. Mitchell, Phys. Rev. B **59**, 3434 (1999).
9. V. E. Fortov, V. Y. Ternovoi, S. V. Kvitov et al., JETP Lett. **69**, 926 (1999).
10. V. E. Fortov, V. Y. Ternovoi, M. V. Zhernokletov et al., JETP **97**, 259 (2003).
11. W. J. Nellis, A. C. Mitchell, P. C. McCandless et al., Phys. Rev. Lett. **68**, 2937 (1992).
12. N. F. Mott, Philos. Mag. **24**, 2 (1971).
13. A. Gedanken, B. Raz, and J. Jortner, J. Chem Phys. **59**, 2752 (1973).
14. K. Inoue, H. Kanzaki, and S. Suga, Sol. St. Comm. **30**, 627 (1980).
15. L. E. Lyons and M. G. Sceats, Chem. Phys. Lett. **6**, 217 (1970).
16. A. M. Ratner, Phys. Rep. **269**, 197 (1996).

17. L. D. Landau and E. M. Lifshits, *Quantum Mechanics*: *Non-relativistic Theory*, Pergamon Press, Oxford (1977).

18. V. V. Zavyalov and I. I. Smolyaninov, JETP Lett. **44**, 182 (1986).

19. I. I. Smolyaninov, Int. J. Mod. Phys. **15**, 2075 (2001).

20. M. W. Cole, Rev. Mod. Phys. **46**, 451 (1974).

21. V. B. Shikin and Y. P. Monarkha, *Two-dimensional Charged Systems in Helium*, Nauka, Moscow (1989).

22. B. Halpern and R. Gomer, J. Chem. Phys. **51**, 1031 (1969).

23. Y. Sakai, E. H. Böttcher, and W. F. Schmidt, J. Jpn. Inst. Electr. Eng. A **61**, 499 (1983).

24. A. A. Levchenko and L. P. Mezhov-Deglin, J. Low Temp. Phys. **89**, 457 (1992).

25. A. A. Levchenko and L. P. Mezhov-Deglin, JETP Lett. **54**, 234 (1991).

26. A. A. Levchenko and L. P. Mezhov-Deglin, Sov. J. Low Temp. Phys. **17**, 229 (1991).

27. A. B. Trusov, L. P. Mezhov-Deglin, and A. A. Levchenko, JETP Lett. **63**, 376 (1996).

28. K. R. Atkins, Phys. Rev. **116**, 1339 (1959).

29. P. C. Soers, E. M. Fearon, P. E. Roberts, R. T. Tsugawa, J. D. Poll, and J. L. Hunt, Phys. Lett. A **77**, 277 (1980).

30. R. L. Brooks, M. A. Selen, J. L. Hunt, J. R. MacDonald, J. D. Poll, and J. C. Waddington, Phys. Rev. Lett. **51**, 1077 (1983).

31. J. A. Forrest and R. L. Brooks, Phys. Rev. B **55**, 906 (1997).

32. J. A. Forrest, J. L. Hunt, and R. L. Brooks, Can. J. Phys. **68**, 1247 (1990).

33. A. A. Zakhidov and K. Yoshino, Synthetic Metals **64**, 155 (1994).

34. T. Miyazaki, K. Yamamoto, and Y. Aratono, Chem. Phys. Lett. **232**, 229 (1995).

35. M. C. R. Symons, Chem. Phys. Lett. **247**, 607 (1995).

36. T. Miyazaki, J. Kumagai, and T. Kumada, Radiat. Phys. Chem. **60**, 381 (2001).

37. W. F. Schmidt, *Liquid State Electronics of Insulating Liquids*, CRC Press, Boca Raton, (1997).

38. A. G. Khrapak, High Temp. **13**, 775 (1975).

39. A. V. Berezhnov, A. G. Khrapak, E. Illenberger, and W. F. Schmidt, High Temp. **41**, 425 (2003).

40. H. A. Bethe and E. E. Salpeter, *Quantum Mechanics of One- and Two-Electron Atoms*, Academic, New York (1957).

41. I. T. Iakubov and A. G. Khrapak, Phys. Rev. A **51**, 5043 (1995).

42. I. T. Iakubov and A. G. Khrapak, Rep. Progr. Phys. **45**, 697 (1982).

43. A. M. Troyanovskii, A. P. Volodin, and M. S. Khaikin, JETP Lett. **29**, 382 (1979).

44. A. M. Troyanovskii and M. S. Khaikin, JETP **54**, 214 (1981).

45. C. Grimes, T. R. Brown, M. L. Burns, and C. L. Zipfel, Phys. Rev. **13**, 140 (1976).

46. A. P. Volodin and V. S. Edelman, JETP Lett. **30**, 633 (1979).

47. M. W. Cole, Phys. Rev. B **2**, 4239 (1970).

48. A. Gedanken, B. Raz, and J. Jortner, Chem Phys. Lett. **14**, 326 (1972).

49. V. Lukin and B. S. Yakovlev, Chem. Phys. Lett. **42**, 307 (1976).

50. U. Sowada and R. A. Holroyd, J. Chem. Phys. **70**, 3586 (1979).

51. A. G. Khrapak and K. F. Volykhin, JETP **88**, 320 (1999).

52. A. G. Khrapak, P. Tegeder, E. Illenberger, and W. F. Schmidt, Chem. Phys. Lett. **310**, 557 (1999).

53. P. D. Grigor'ev and A. M. Dyugaev, JETP **88**, 325 (1999).

54. J. A. Forrest et al., Phys. Rev. B **46**, 13820 (1992).